Biomechanical reinforcement by CAD-CAM materials affects stress distributions of posterior composite bridges

DOI:
10.1016/j.dental.2024.04.001

Citation for published version (APA):
Elraggal, A., Abdelraheem, I. M., Watts, D. C., Roy, S., Dommeti, V. K., Alshabib, A., Althaqafi, K. A., & Afifi, R. R. (2024). Biomechanical reinforcement by CAD-CAM materials affects stress distributions of posterior composite bridges: 3D finite element analysis. *Dental Materials*, *40*(5), 869-877. https://doi.org/10.1016/j.dental.2024.04.001

Published in:
Dental Materials

Dental Materials 40 (2024) 869–877

Contents lists available at ScienceDirect

Dental Materials

journal homepage: www.elsevier.com/locate/dental

Biomechanical reinforcement by CAD-CAM materials affects stress distributions of posterior composite bridges: 3D finite element analysis.

Alaaeldin Elraggal [a,b,*], Islam M. Abdelraheem [b], David C. Watts [a], Sandipan Roy [c], Vamsi Krishna Dommeti [c], Abdulrahman Alshabib [d], Khaled Abid Althaqafi [e], Rania R. Afifi [b]

[a] Division of Dentistry, School of Medical Sciences, Faculty of Biology, Medicine and Health, The University of Manchester, Manchester, UK
[b] Conservative Dentistry Department, Faculty of Dentistry, Alexandria University, Alexandria, Egypt
[c] Department of Mechanical Engineering, SRM Institute of Science and Technology, Kattankulathur 603203, Tamil Nadu, India
[d] Restorative Dentistry Department, Faculty of Dentistry, King Saud University, Riyadh, Saudi Arabia
[e] Restorative Dentistry Department, Faculty of Dentistry, College of Dental Medicine, University of Umm Al Qura, Makkah, Saudi Arabia

ARTICLE INFO

Keywords:
Finite element analysis
Immediate composite bridges
Zirconia
Lithium disilicate
Trilor
PEEK

ABSTRACT

Objectives: This 3D finite element analysis study aimed to investigate the effect of reinforcing CAD-CAM bars on stress distribution in various components of a posterior composite bridge.
Methods: A virtual model mimicking the absence of an upper second premolar was created, featuring class II cavity preparations on the proximal surfaces of the adjacent abutment teeth surrounding the edentulous space. Five distinct finite element analysis (FEA) models were generated, each representing a CAD-CAM reinforcing bar material: 3-YTZP (IPS. emax ZirCAD MO; Zr), lithium disilicate (IPS e.max CAD; EX), nano-hybrid resin composite (Grandio Blocs; GB), Fibre-reinforced composite (Trilor; Tri), and polyetheretherketone (PEEK). A veneering resin composite was employed to simulate the replacement of the missing premolar (pontic). In the FEA, an axial force of 600 N and a transverse load of 20 N were applied at the center of the pontic. Subsequently, maximum von Mises (mvM) and maximum principal stresses (σmax) were computed across various components of the generated models. Additionally, shear stresses at the interface between the CAD-CAM bars and the veneering resin composite were determined.
Results: CAD-CAM materials with high modulus of elasticity, such as Zr and EX, exhibited the highest mvM stresses and shear stresses while transferring the lowest stress to the veneering resin composite in comparison to other materials. Conversely, PEEK demonstrated the lowest mvM stresses but produced the highest stresses within the veneering resin composite. There was a uniform distribution of mvM stresses in the remaining tooth structure among all groups, except for a noticeable elevation in the molar region of Zr and EX groups.
Significance: Reinforcing CAD-CAM bar materials with a high modulus of elasticity, such as Zr and EX, may result in debonding failures at the connector sites of posterior composite bridges. Conversely, GB, PEEK, and Tri have the potential to cause fracture failures at the connectors rather than debonding.

1. Introduction

The absence of upper permanent premolars can cause distress for patients as it affects both the aesthetics and function within a prominent area of the smile [1]. Various restorative solutions are available for such cases, including removable partial dentures, 3-unit fixed dental bridges (FDB) [2], resin-bonded bridges [3] (RBB), and dental implants [4,5]. However, each of these treatment options comes with its set of limitations, encompassing factors such as patient preferences, tooth structure damage, potential lab errors, time constraints, financial considerations, requirement for surgical procedures, and retention reliability [6–8].

The immediate replacement of a permanent tooth has been promoted through techniques using fiber-reinforced resin composites or bonding the extracted natural tooth to its neighboring one [9,10]. This immediate restorative approach offers benefits such as excellent aesthetics, the capacity to bond to tooth structure, minimal invasiveness, and easy repair if needed [11]. Immediate fibre-reinforced composite bridges (FCB), described in the literature, have been recognized as a durable and

* Corresponding author at: Division of Dentistry, School of Medical Sciences, Faculty of Biology, Medicine and Health, The University of Manchester, Manchester, UK.
E-mail address: Alaadin.elraggal@Manchester.ac.uk (A. Elraggal).

https://doi.org/10.1016/j.dental.2024.04.001
Received 17 February 2024; Received in revised form 28 March 2024; Accepted 2 April 2024
Available online 11 April 2024

more conservative means of replacing a missing anterior tooth compared to traditional fixed bridges or implant-supported crowns [12–14]. However, immediate FCB have exhibited unsatisfactory clinical performance, with only a 75% success rate over the initial 5 years [15]. A prevalent failure is delamination between resin composites and reinforcing fibers [16]. Mechanical tests indicate that fractures primarily occur at the interface between the resin composite and fibers, loading points, and connectors [17,18]. Occlusal forces can cause fiber bending, generating combined shear and tensile forces between the reinforcing fibers and veneering resin composite [19]. Exceeding the bond strength between these dissimilar materials due to tensile and shear forces can lead to debonding and hence a collapse of the whole restoration.

Advancements in CAD-CAM materials have expanded clinicians' choices for dependable restorative materials boasting excellent aesthetics and optimal mechanical properties. CAD-CAM resin composites [20], lithium disilicate glass ceramics [21], hybrid ceramics [22], polycrystalline zirconia [23], and PEEK [24] find broad applications in restorative dentistry, manufactured under isostatic conditions to ensure exceptional mechanical performance. CAD-CAM blocks are commonly milled into indirect restorations like crowns, bridges, onlays, and veneers, later bonded to tooth structure using adhesive resins [25]. Existing literature demonstrates their enduring, strong bonds with resin composites, provided proper mechanical and chemical surface treatments are applied [26–28]. However, these materials have not been widely explored as potential reinforcing frameworks for immediate posterior composite bridges. Finite Element Analysis (FEA) has emerged as a valuable tool in bioengineering, offering computational modeling capabilities to explore the impact of various design variables across diverse fields of restorative dentistry. FEA enables researchers to simulate complex scenarios and investigate the effects of different parameters, such as stress distribution, orientation, and deformation, in virtual designs of fixed partial dentures [29,30]. By utilizing FEA, researchers can map out stress patterns and evaluate the structural integrity of dental restorations under different loading conditions, providing valuable insights for optimizing design parameters and enhancing clinical performance [31].

The immediate replacement of a missing posterior tooth represents a cost-effective innovation that is less invasive to neighboring teeth, potentially repairable using direct resin composites, and generally more affordable than traditional treatment methods. This approach offers a timely solution for replacing a single tooth when extraction is necessary. The study posits that CAD-CAM reinforcing framework bars might establish a more favorable mechanical interaction with the veneering resin composite. However, this theoretical interaction remains untested and unverified. Therefore, the objective of the present study is to investigate the effect of reinforcing CAD-CAM bar materials and its stress distribution in various components of a posterior composite bridge using finite element analysis. The study's null hypotheses encompass two aspects: first, that various CAD-CAM materials (such as resin composite, 3-YTZP, lithium disilicate, PEEK, and fiber-reinforced resin) will not impact stress distributions in both the veneering resin composite restoration and tooth structure (enamel and dentin); and second, that there will be no disparity in stress distribution among the different reinforcing CAD-CAM materials.

2. Materials and methods

Finite element analysis and Weibull probability failure were conducted to investigate the stress distributions and probability of fracture of five models generated for different immediate posterior composite bridge reinforced with five CAD-CAM materials (1- IPS e.max ZirCAD 3-YTZP zirconia; Ivoclar Vivadent AG, Schann, Liechtenstein [Zr], 2- Grandio blocs; VOCO, Germany [GB], and 3- Fibre-reinforced composite Trilor; Harvest Dental, Brea, CA [Tri], 4- Polyetherether ketone PEEK-OPTIMA®; Invibio, UK [PEEK], and 5- IPS e.max CAD Lithium Disilicate blocks; Ivoclar Vivadent AG, Schann, Liechtenstein [EX]. This work was approved by the ethics committee of the Faculty of Dentistry Research Ethics (International No: IORG0008839).

2.1. CAD-CAM reinforced composite bridge model design

A finite element analysis model was constructed, featuring an upper first permanent premolar and molar set 6 mm apart within type 4 bone. Computerized tomography (CT) scans of actual human premolar and molar teeth were utilized to capture precise dimensions and shapes for the model. A standard representation of a posterior CAD-CAM reinforced composite bridge was assembled using one of five CAD-CAM bar materials, each set at specific dimensions (2 mm wide, 12 mm long, and 1 mm thick). These bars were positioned within proximal box-shaped cavities between the premolar and molar, embedded within a veneering resin composite material that extended to fill the proximal boxes of the two teeth (Fig. 1). The dimensions of the simulated proximal cavities adhered to recommendations from prior studies [18,19]. The model assumes perfect bonding at all interfaces within the composite bridge, encompassing connections between the CAD-CAM bars and veneering resin composite, as well as those between the resin composite and the structures of the teeth (enamel and dentin).

2.2. Model generation

The obtained data was exported and superimposed into interactive medical image control using Digital Imaging and Communications in Medicine format (DICOM) to detect the boundaries of the remaining tooth structure, pulp chamber, etc. A reverse engineering program (Mimics Medical 20.0; Materialize NV and Geomagic Studio 12.0; Geomagic Inc) was used to translate the scanned data into full CAD 3D models. Veneering resin composite was designed using 3Shape Dental Designer CAD software (inLab 3D software). Five models were generated according to the five CAD-CAM reinforcing bar materials. Veneering composite was designed with ExoCAD software version 4.3 (Sirona Dental Systems, Bensheim, Germany) according to the original anatomy of an upper second premolar.

Following an initial scanning process, the obtained models were converted into.stl files and subsequently imported into the geometry section of Ansys 2023 R2. Specific components, such as pre-molar, molar, restoration, and a bar featuring a length of 12 mm and a rectangular cross-section measuring 2 mm x 1.5 mm, were extracted from the scan data. Within the ANSYS Workbench Space Claim environment, additional elements like cortical, sized at 45 mm x 35 mm, were generated. A cancellous component was created separately as a solid with a thickness of 2 mm. The Boolean operations feature in Space Claim, specifically the combine option, was employed to establish the periodontal ligament with a thickness of 0.2 mm. In a similar fashion, the pulp and enamel components, each with a solid thickness of 1.5 mm, were individually created using the split command in Space Claim. The entire assembly, as depicted in Fig. 1(b), from Space Claim, was then imported into the model module.

To facilitate interactions within the model, contact bodies and target bodies were established between various geometry sections. Specifically, contacts were formed between enamel and dentin, dentin and periodontal ligament, periodontal ligament and cancellous, and cancellous and cortical interfaces. A total of 24 contacts were configured, all set as bonded conditions.

Conducting a comprehensive convergence study, the overall model was meshed with a 0.5 mm element size using the solid 187 element type. Each geometric model was subjected to meshing, resulting in a total of 3463,350 nodes and 3117,240 elements within the entire assembly.

Boundary conditions play a pivotal role in FEA by defining node movements and relationships. The following conditions were upheld across all models:

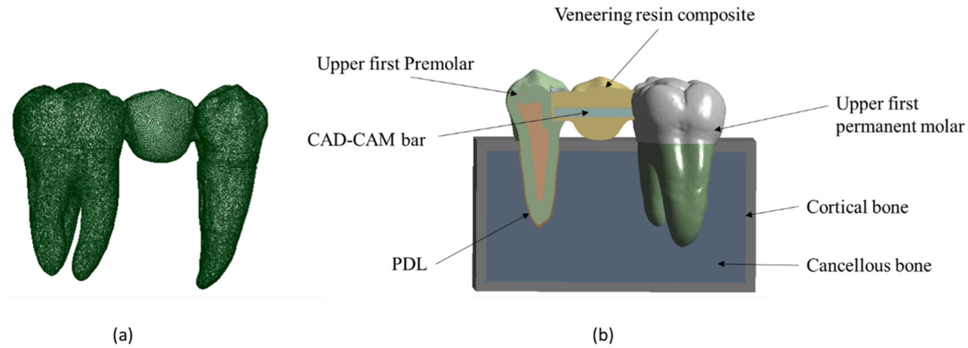

Fig. 1. a) 3D FE model showing the mesh densities of posterior CAD-CAM reinforced bridge replacing an upper second premolar tooth. b) A sectional view showing the 3D FE model showing the location of the reinforcing CAD-CAM bar near the ginigival steps of a distal box of an upper first permanent premolar and a mesial box on an upper first permanent molar. A veneering resin composite surrounds the CAD-CAM bar and fills between the two proximal boxes and is shaped to simulate an upper second permanent premolar.

(1) All materials within the models were uniform, isotropic, and exhibited linear elasticity.

(2) FEA models were firmly positioned within the alveolar bone, restricted from movement (0° freedom in all directions) to prevent any rigid body motion.

(3) Boundary conditions were applied consistently across nodes, ensuring no flaws existed in any Finite element analysis.

Material properties of all components of the FEA model are presented in Table 1. It was assumed that all components had isotropic material properties except for the reinforcing CAD-CAM bar materials.

Despite the physiological occlusal forces averaging 200 N in the premolar region, a load of 600 N was applied axially to the central occlusal surface of the virtual pontic of an upper second permanent premolar, representing a worst-case scenario. Additionally, a transverse force of 200 N was directed at a 45-degree angle to the long axis of the model, toward the palatal inclination of the palatal cusp [42,43] (Fig. 2).

The stress patterns for various models were calculated using computer-aided software, ANSYS 2023 (ANSYS Inc., Canonsburg, Pennsylvania, United States). A linear static Finite Element Analysis (FEA) was utilized to assess the strength of materials under complex stress conditions. The evaluation included analyzing the maximum von Mises (mvM) stresses and maximum principal stresses (σmax) on the enamel, dentine, reinforcing CAD-CAM bar, and veneering resin composite, measured in megapascals (MPa). Additionally, an assessment was conducted on the tensile and shear forces occurring at the interface between the CAD-CAM bar and the resin composite.

The numerical data generated by the FEA was represented graphically in color, where similar colors indicated similar stress distribution ranges. Warmer colors indicated higher stresses, with red areas representing the highest stress concentrations, while blue areas denoted lower stresses. Each component of the FEA was extracted and sectioned mesio-distally to examine the stress patterns in individual components.

components of the models.

Table 1
Elastic properties of the isotropic materials used for the FE analysis.

Material	Elastic modulus (GPa)	Poisson ratio
Enamel[32]	84.10	0.30
Dentin[32]	18.60	0.31
Periodontal ligament[33]	0.0689	0.45
Cortical bone[34]	13.70	0.30
Trabecular bone[34]	1.37	0.30
Resin composite[35]	15.5	0.28
IPS e.max CAD[36]	102.70	0.33
PEEK[37]	4.8	0.36
Trilor[38]	26	0.3
Grandio Blocs[39]	18	0.26
IPS e.max ZirCAD MT[40,41]	210	0.30

3. Results

Quantitative data regarding mvM and σmax for distinct model components were detailed in Table 2 and Table 3, correspondingly. These findings were also visually represented as bar charts in Fig. 3 and Fig. 4. The sectional views in Figs. 5–8 depicted the stress distribution among various components of the FEA model. The color spectrum ranging from red (indicating the highest stress concentration) to blue (suggesting lower stress levels) demonstrated the stress gradients across these sections. Stress values within a 5% difference were considered analogous.

In general, within the FEA model, the highest mvM and σmax were observed in the enamel structure of the premolar, followed by the molar abutment. Notably, the veneering resin composite pontic exhibited the third-highest mvM and σmax across various reinforcing CAD-CAM materials. However, for Zr, the stresses were elevated in the CAD-CAM zirconia bar compared to the veneering resin composite.

3.1. Stress distribution in the CAD-CAM bars and veneering resin composite

In the mvM distribution of the reinforcing CAD-CAM bars (Fig. 5**a-e**), the FEA revealed the zones of maximum stress concentration at the connectors where the CAD-CAM bars link the pontic to either the molar or premolar, particularly at the apical side of the bar. Stress levels ranged from lower values in PEEK (31.3 MPa) to higher levels in GB, Tri, and EX (52.5, 59.9, and 113.4 MPa, respectively), while mvM stresses peaked at 154.9 MPa in Zr.

In the mvM stress distribution within the veneering resin composite (depicted in Fig. 6), the FEA highlighted maximum stress concentrations at the areas of loading for all models. These stresses were concentrated where the load was applied, and the mvM stress in the resin composite pontic displayed a radial pattern emanating from the loaded area. Apart from the small region around the point of loading, the stresses spread radially and concentrated at the top and bottom of the connectors across all groups. The highest mvM concentration was observed in the PEEK group (187.2 MPa), followed by GB, Tri, and EX groups (152.4, 144.5, 126.7 MPa, respectively), whereas the lowest von Mises values were noted in the Zr group (118.2 MPa). The areas of the highest mvM were broader in PEEK and GB compared to the other groups. Similar trends were observed in σmax values, with the highest σmax in PEEK (115 MPa) and the lowest σmax in Zr (56.5 MPa).

Shear stresses, generated at the interface between CAD-CAM bar and resin composite, are illustrated in Fig. 7. The highest shear stresses were identified in Zr and EX (89.3 MPa and 65.4 MPa, respectively), while the PEEK group exhibited the lowest stresses (18 MPa). Both GB and Tri groups demonstrated nearly equivalent shear stresses (30.3 and 34.5 MPa, respectively). In each group, the highest shear stresses are

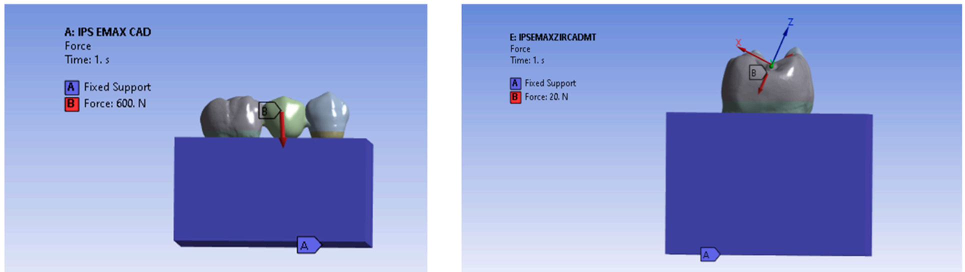

(a) Axial Load (b) Transverse load

Fig. 2. boundary conditions with (a) Axial Load (b) Transverse load.

Table 2
von Mises in MPa among different tooth substrates (enamel and dentin) of the premolar and molar, resin composite pontic, and the reinforcing CAD-CAM bar materials.

Bar Martial	Dentin (premolar)	Dentin (molar)	Resin composite	Bar
IPS e.max CAD	36.9	80.7	126.7	113.4
PEEK	40.3	32.8	187.2	31.3
Trilor	37.9	42.5	144.5	59.9
Grandio Blocs	38.5	40.8	152.4	52.5
IPS e.max ZirCAD MT	36.4	91.9	118.2	154.9

Table 3
Maximum principal stresses in MPa among different tooth substrates (enamel and dentin) of premolar and molar, resin composite pontic, and the reinforcing CAD-CAM bar materials.

Bar Martial	Dentin (premolar)	Dentin (molar)	Resin composite	Bar
IPS e.max CAD	12.1	44.4	62.5	61.9
PEEK	14.9	14.8	115.0	18.7
Trilor	13.2	32.1	80.6	30.9
Grandio Blocs	13.5	28.4	87.1	28.1
IPS e.max ZirCAD MT	12.4	58.3	56.5	91.9

primarily confined to the underside of the CAD-CAM bar, except for a more dispersed pattern observed on the upper surface of the Zr and EX groups.

3.2. Stress distribution in the remaining (dentin) tooth structure) of the abutments (premolar and molar)

von Mises stress distributions in dentin of molar and premolar for different CAD-CAM bar materials are illustrated in Fig. 8 **a-e** and Fig. 8 **f-j**, respectively. von Mises stress distributions in the molar were generally higher, compared to the premolar, in all CAD-CAM bars except for PEEK; the mvM were higher in premolar. The mvM were found in molar of Zr (91.9 MPa) followed by molar of EX (80.7 MPa) while the lowest von Mises were found in the molar of PEEK (32.8 MPa). The stresses were concentrated at the cervical margin of the two proximal boxes and radiated in an apical and bucco-palatal directions. The highest von Mises extended more apically in the premolar compared to the molar where the maximum stresses gradually faded towards the middle of the roots.

4. Discussion

The immediate replacement of a missing upper premolar is a cost-effective and conservative alternative to conventional fixed-fixed bridges or implant-supported coronal restorations. Nevertheless, this method needs to be dependable and meet the essential requirements for a successful prosthesis. This study aimed to assess and contrast various reinforcing CAD-CAM bar materials concerning stress dispersion in a resin composite-made veneering pontic and the remaining tooth structure. Significant variations in stress distribution were observed among each CAD-CAM bar material and within the veneering resin composite, thereby leading to the rejection of the null hypotheses.

Finite element analysis serves as a valuable tool for assessing the strengths and weaknesses of fixed restoration components and understanding the potential stresses they may encounter under diverse loads

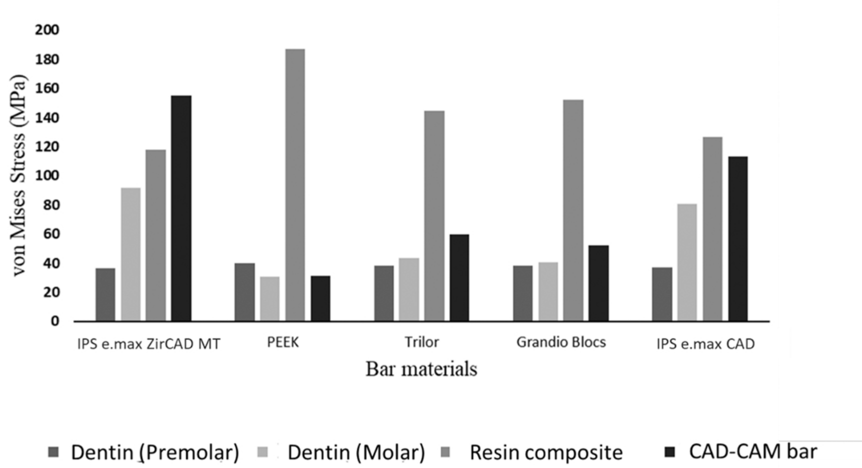

Fig. 3. von Mises stress distribution (MPa) for different of different tooth substrates, resin composite, and reinforcing CAD-CAM bar materials in each of the study groups.

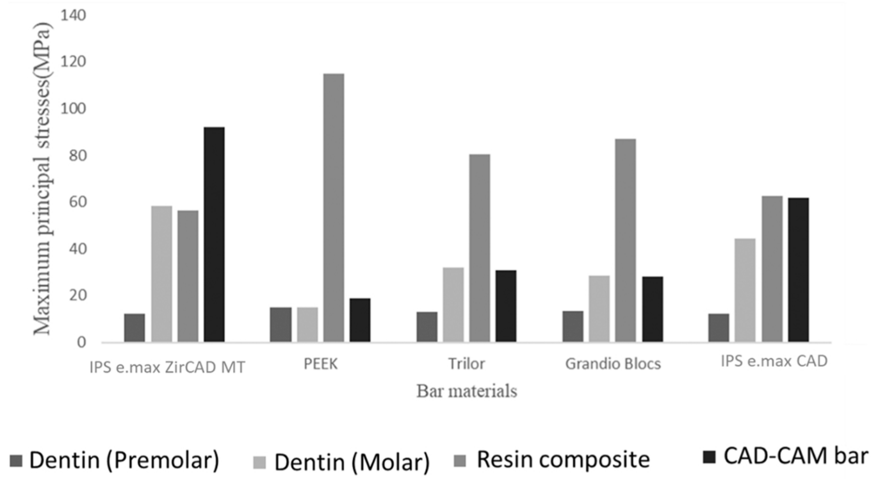

Fig. 4. Maximum principal stresses (MPa) for different tooth substrates, resin composite, and reinforcing CAD-CAM bar materials in each of the study groups.

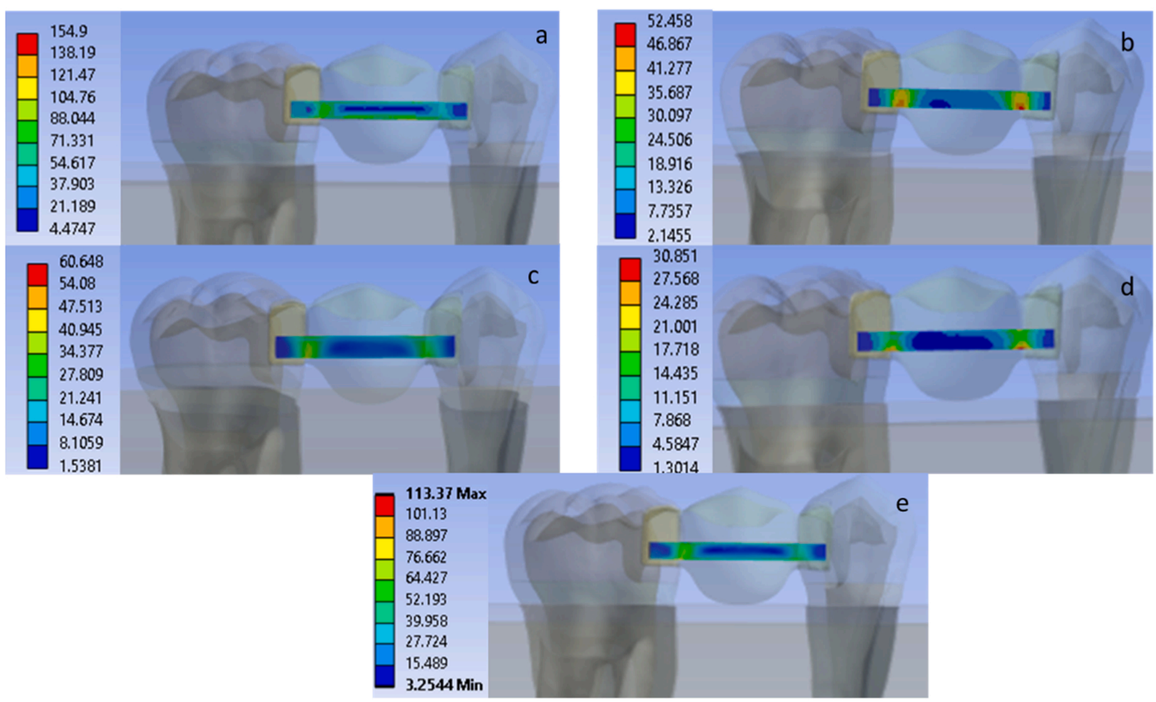

Fig. 5. von Mises stress distribution (MPa) among reinforcing CAD-CAM bar materials with a-e correspond to IPS e.max ZirCAD, Grandio Blocs, Trilor, PEEK, and IPS e.max CAD, respectively.

[44]. Through this analysis, we can evaluate how these components affect stress distribution in different substrates, providing insights into the potential clinical success of dental restorations [45]. This study developed a 3D finite element analysis model featuring a box-shaped CAD-CAM reinforced posterior composite bridge, serving as a replacement for an upper second permanent premolar. Similar box-shaped designs have been recommended in prior research where authors assessed fibre-reinforced composite bridges through FEA methods [18, 19] or explored inlay-retained bridges [46,47].

The application of adhesive prostheses in dentistry serves as a less invasive alternative to more aggressive treatments [48]. Thanks to advancements in dental adhesives, the cementation of extensive restorations and fixed prostheses has become more accessible and is recommended for achieving favorable success rates over a period of five years, demonstrating comparable performance to conventional fixed dental prostheses or implant-supported crowns [49]. This shift towards adhesive dental bridges aligns with minimally invasive dentistry, reducing the need for substantial abutment tooth preparation to support fixed prostheses. Hence, the present study simulated a minimal preparation model, where each adjacent tooth to the edentulous space underwent only one class II preparation for a direct approach of fixed partial denture.

Physiological occlusal loads can differ according to the magnitude of functional and parafunctional activities. The maximum occlusal forces, in the posterior region, can reach up to 580 N [50,51]. In the current FEA study model, a magnitude of 600 N was applied to mimic the worst case scenario on posterior teeth [52].

Advancements in CAD-CAM material development have significantly broadened the range of options available to clinicians in restorative dentistry. These materials can be utilized either as a complete restoration or as a foundational material to support an aesthetic restoration. Among the materials commonly used are 3-YTZP zirconia, lithium

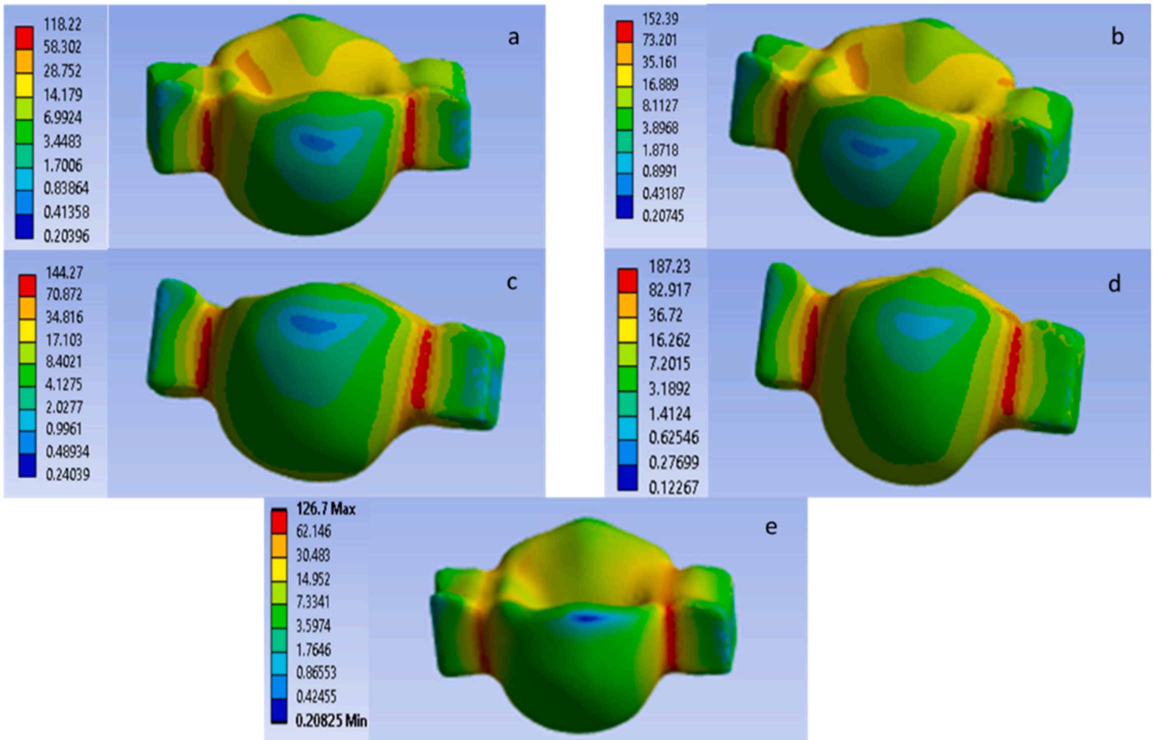

Fig. 6. von Mises stress distribution (MPa) for the veneering resin composite among the different reinforcing CAD-CAM bar materials with a-e correspond to IPS e.max ZirCAD, Grandio Blocs, Trilor, PEEK, and IPS e.max CAD, respectively.

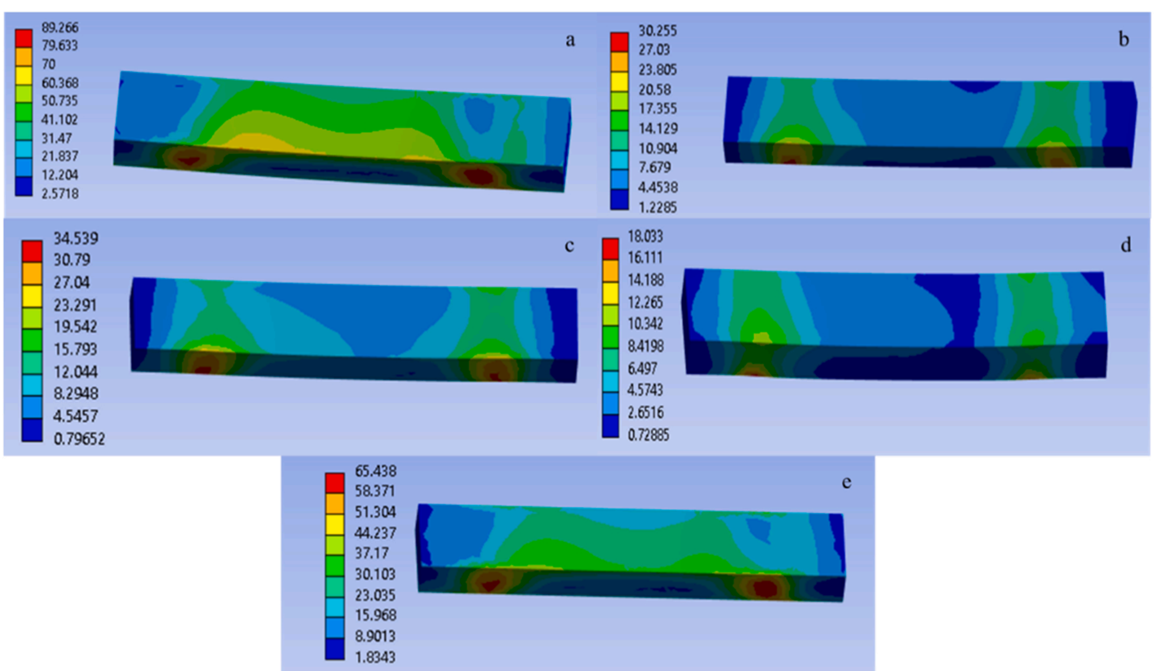

Fig. 7. Shear stresses generated at the interface between the veneering resin composite and different CAD-CAM bar materials (a-e) corresponding to IPS e.max ZirCAD, Grandio Blocs, Trilor, PEEK, and IPS e.max CAD, respectively.

disilicate, PEEK, fibre-reinforced composites, and nanohybrid resin composites, known for their outstanding mechanical properties [38, 53–55] In Fibre-reinforced composite bridges, the most common failure site was at the connectors [17,56] In this FEA study, these materials were considered as potential CAD-CAM reinforcing bar materials, aiming to achieve favorable stress distribution, reduce fracture risks, and extend the lifespan of a posterior composite bridge. The premise behind this approach was that reinforcing a posterior composite bridge with high elastic modulus CAD-CAM materials would withstand the stresses at the connector areas, consequently minimizing the likelihood of fracture, as agreed by a previous work [57].

The study revealed varying stress concentrations among different

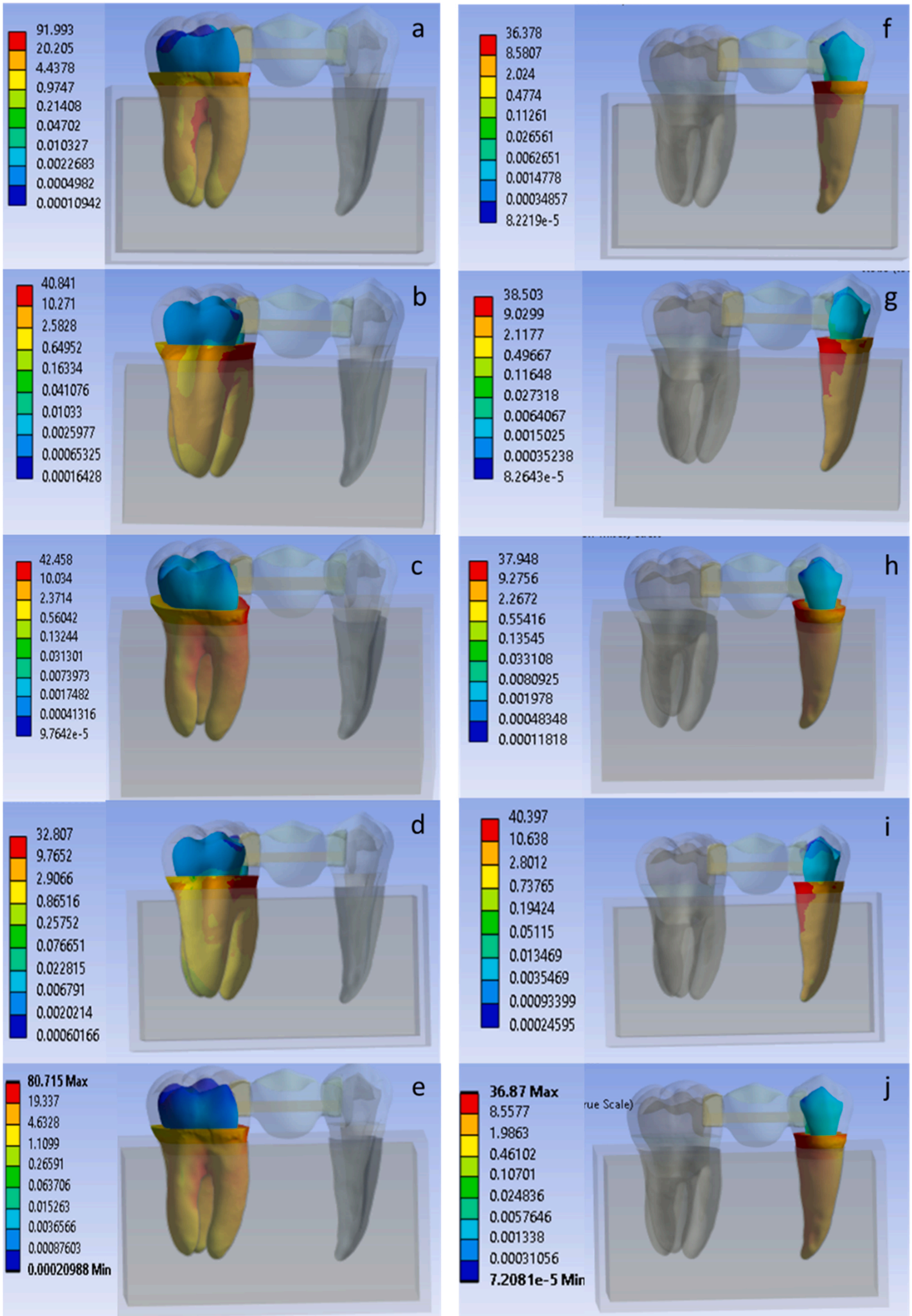

Fig. 8. von Mises stress distribution (MPa) among the dentin structure in molar abutment (a-e) and premolar abutment (f-j). Figures (a-e) and (f-j) correspond to the different CAD-CAM bar materials; IPS e.max ZirCAD, Grandio Blocs, Trilor, PEEK, and IPS e.max CAD, respectively.

CAD-CAM materials, primarily influenced by their modulus of elasticity and Poissons ratio in the analytical conditions. In comparison to IPS e.max CAD and IPS e.max ZirCAD, PEEK, Grandio Blocs, and Trilor have lower modulus of elasticity. The resilient properties of PEEK, Grandio Blocs, and Trilor allow them to absorb forces, creating flexible restorations akin to natural teeth, aligning with previous research [58,59].

The veneering resin composite exhibited the highest von Mises stress concentrations in the PEEK group (187.2 MPa). This disparity may be attributed to PEEK's relatively low elastic modulus (4.8 MPa) in contrast to the veneering resin composite (15.5 GPa). This mismatch permits PEEK to deform under occlusal loads, potentially transmitting higher stresses to the veneering composite. This phenomenon can potentially lead to catastrophic tooth fractures or restoration debonding, consistent with previous studies [45,60].

Conversely, Zr and EX, being more rigid materials, display higher stress resistance but may undergo catastrophic failure under excessive loads surpassing their fracture resistance, as observed in prior research [61]. Zirconia and Lithium disilicate materials might have effectively absorbed more stresses than PEEK, transferring lesser stress to substrates with lower modulus of elasticity, aligning with findings by Yamanel et al. [45]. The outcomes are in line with the mvM stress findings in CAD-CAM bar materials, where Zirconia (Zr) and Emax (EX) displayed the highest stress values (154.9 MPa and 113.37 MPa, respectively), while PEEK exhibited the lowest stress level (31.3 MPa). Trilor and Grandio Blocs showed higher mvM (59.9 MPa and 52.45 MPa, respectively) compared to PEEK, transferring less stresses to the veneering resin composite (144.45 MPa and 152.4 MPa, respectively).

The study findings revealed that the stress concentration at the adhesive interface is influenced by the elastic modulus of the CAD-CAM material [47,62]. The highest shear stresses, at the interface between CAD-CAM bar and veneering resin composite, were found in groups Zr and EX, while the lowest stresses were found in PEEK. CAD-CAM materials with high modulus of elasticity such as Zr and EX enable high shear stresses at the adhesive/restoration interface with increased risk for debonding. These restorations tend to debond rather than cause a fracture to the remaining tooth structure as agreed by [47,52,63].

The CAD-CAM bar materials exhibited comparable mvM stresses transmitted to the remaining tooth structure, regardless of whether it was in the molar or premolar region. This uniform stress distribution might stem from the identical dimensions of the class II cavities in both abutments, leading to a similar C-factor, a concept supported by prior research [47]. Nonetheless, there was a marginal elevation in mvM stresses observed in the molars, particularly evident in the Zr_{molar} and EX_{molar} groups compared to other CAD-CAM bars. However, the uneven distribution of stress in the Zr_{molar} and EX_{molar} groups might be attributed to the higher stress transfer capacity of materials with elevated modulus of elasticity, particularly when located proximate to the cervical gingival step within the class II cavity.

Finite element analysis is a mathematical technique that, while useful, doesn't comprehensively mirror the multifaceted aspects found in real clinical scenarios. It overlooks crucial parameters that may impact the durability of CAD-CAM reinforced bridges, such as the integrity of the periodontium, bone density, thermal expansion coefficients of the components under examination, dentoalveolar responses to various functional loads, and the intricate and dynamic nature of mastication physiology. To obtain more dependable and practical data to confirm the efficacy of CAD-CAM reinforced posterior composite bridges, additional mechanical laboratory testing and extensive long-term clinical trials are warranted.

5. Conclusions

1. Rigid materials such as 3-YTZP zirconia and lithium disilicate showed the highest von Mises within the CAD-CAM reinforcing material but the lowest in the veneering composite.
2. 3-YTZP and lithium disilicate materials can better absorb the occlusal stresses but generate higher shear stresses increasing the risk of debonding. However PEEK, Trilor, and Grandio Blocs transfer higher stresses to the veneering resin composite indicating higher risk for fracture

Declaration of Competing Interest

The authors have no competing interests to declare.

References

[1] Naoum S, Allan Z, Yeap CK, Razza JM, Murray K, Turlach B, et al. Trends in orthodontic management strategies for patients with congenitally missing lateral incisors and premolars. Angle Orthod 2021;91:477–83.
[2] Forrer FA, Schnider N, Brägger U, Yilmaz B, Hicklin SP. Clinical performance and patient satisfaction obtained with tooth-supported ceramic crowns and fixed partial dentures. J Prosthet Dent 2020;124:446–53.
[3] Balasubramaniam GR. Predictability of resin bonded bridges - a systematic review. Br Dent J 2017;222:849–58.
[4] Hickel R, Brüshaver K, Ilie N. Repair of restorations–criteria for decision making and clinical recommendations. Dent Mater 2013;29:28–50.
[5] Staehle HJ, Sekundo C, Hieronymus H, Büsch C, Frese C. Replacing single missing teeth in the posterior region using direct composite restorations: Survival and clinical quality. J Dent 2021;113:103754.
[6] Pankratz V, Zimmer S, Marković L. Anterior fiber-reinforced ribbon composite resin bridge—A case report. Clin Case Rep 2018;6:1941–6.
[7] Antonarakis GS, Prevezanos P, Gavric J, Christou P. Agenesis of maxillary lateral incisor and tooth replacement: cost-effectiveness of different treatment alternatives. Int J Prosthodont 2014;27:257–63.
[8] Di Fiore A, Meneghello R, Graiff L, Savio G, Vigolo P, Monaco C, et al. Full arch digital scanning systems performances for implant-supported fixed dental prostheses: a comparative study of 8 intraoral scanners. J Prosthodont Res 2019; 63:396–403.
[9] Tanoue N, Matsumura H, Yamamori T, Ohkawa S. Longevity of resin-bonded fixed partial dentures made of metal alloys: A review of the literature. J Prosthodont Res J Jpn Prosthodont Soc 2021.
[10] Ahmed KE, Li KY, Murray CA. Longevity of fiber-reinforced composite fixed partial dentures (FRC FPD)—Systematic review. J Dent 2017;61:1–11.
[11] Burke FJT. Resin-retained bridges: fibre-reinforced versus metal. Dent Update 2008;35:521–2. 524–6.
[12] Wolff D, Schach C, Kraus T, Ding P, Pritsch M, Mente J, et al. Fiber-reinforced composite fixed dental prostheses: a retrospective clinical examination. J Adhes Dent 2011;13:187–94.
[13] Frese C, Schiller P, Staehle HJ, Wolff D. Fiber-reinforced composite fixed dental prostheses in the anterior area: a 4.5-year follow-up. J Prosthet Dent 2014;112: 143–9.
[14] Escobedo Martínez MF, Rodríguez López S, Valdés Fontela J, Olay García S, Mauvezín Quevedo M. A New Technique for Direct Fabrication of Fiber-Reinforced Composite Bridge: A Long-Term Clinical Observation. Dent J 2020;8:48.
[15] Vallittu PK. Survival rates of resin-bonded, glass fiber-reinforced composite fixed partial dentures with a mean follow-up of 42 months: a pilot study. J Prosthet Dent 2004;91:241–6.
[16] Göhring TN, Roos M. Inlay-fixed partial dentures adhesively retained and reinforced by glass fibers: clinical and scanning electron microscopy analysis after five years. Eur J Oral Sci 2005;113:60–9.
[17] Kolbeck C, Rosentritt M, Behr M, Lang R, Handel G. In vitro examination of the fracture strength of 3 different fiber-reinforced composite and 1 all-ceramic posterior inlay fixed partial denture systems. J Prosthodont 2002;11:248–53.
[18] Song H-Y, Yi Y-J, Cho L-R, Park D-Y. Effects of two preparation designs and pontic distance on bending and fracture strength of fiber-reinforced composite inlay fixed partial dentures. J Prosthet Dent 2003;90:347–53.
[19] Shi L, Fok ASL. Structural optimization of the fibre-reinforced composite substructure in a three-unit dental bridge. Dent Mater 2009;25:791–801.
[20] Peampring C. Restorative management using hybrid ceramic of a patient with severe tooth erosion from swimming: a clinical report. J Adv Prosthodont 2014;6: 423–6.
[21] Della Bona A, Corazza PH, Zhang Y. Characterization of a polymer-infiltrated ceramic-network material. Dent Mater 2014;30:564–9.
[22] Sonmez N, Gultekin P, Turp V, Akgungor G, Sen D, Mijiritsky E. Evaluation of five CAD/CAM materials by microstructural characterization and mechanical tests: a comparative in vitro study. BMC Oral Heal 2018;18:1–13. 181 2018.
[23] Fathy SM, Al-Zordk W, E Grawish M, V Swain M. Flexural strength and translucency characterization of aesthetic monolithic zirconia and relevance to clinical indications: A systematic review. Dent Mater 2021;37:711–30.
[24] Zoidis P, Bakiri E, Polyzois G. Using modified polyetheretherketone (PEEK) as an alternative material for endocrown restorations: A short-term clinical report. J Prosthet Dent 2017;117:335–9.
[25] Chockattu SJ, Deepak BS, Sood A, Niranjan NT, Jayasheel A, Goud MK. Management of dental erosion induced by gastro-esophageal reflux disorder with direct composite veneering aided by a flexible splint matrix. Restor Dent Endod 2018;43.

[26] Elraggal A, Silikas N. Effect of air-abraded versus laser-fused fluorapatite glass-ceramics on shear bond strength of repair materials to zirconia. Materials 2021;14:1468.
[27] Elraggal A, Chen X, Silikas N. Effect of sandblasting with fluorapatite glass-ceramic powder and chemical primers/adhesives on shear bond strength of indirect repairing composite to zirconia. Oper Dent 2022;47:574–84.
[28] Rosentritt M, Preis V, Behr M, Sereno N, Kolbeck C. Shear bond strength between veneering composite and PEEK after different surface modifications. Clin Oral Investig 2015;19:739–44.
[29] Gloria A, Maietta S, Martorelli M, Lanzotti A, Watts DC, Ausiello P. FE analysis of conceptual hybrid composite endodontic post designs in anterior teeth. Dent Mater 2018;34:1063–71.
[30] Ausiello P, Gloria A, Maietta S, Watts DC, Martorelli M. Stress distributions for hybrid composite endodontic post designs with and without a ferrule: FEA study. Polymers 2020;12:1836.
[31] Magne P, Perakis N, Belser UC, Krejci I. Stress distribution of inlay-anchored adhesive fixed partial dentures: A finite element analysis of the influence of restorative materials and abutment preparation design. J Prosthet Dent 2002;87:516–28.
[32] Lin CL, Chang YH, Pa CA. Estimation of the risk of failure for an endodontically treated maxillary premolar with MODP preparation and CAD/CAM ceramic restorations. J Endod 2009;35:1391–5.
[33] Eskitaşcioğlu G, Belli S, Kalkan M. Evaluation of two post core systems using two different methods (fracture strength test and a finite elemental stress analysis). J Endod 2002;28:629–33.
[34] Asmussen E, Peutzfeldt A, Sahafi A. Finite element analysis of stresses in endodontically treated, dowel-restored teeth. J Prosthet Dent 2005;94:321–9.
[35] El-Safty S, Akhtar R, Silikas N, Watts DC. Nanomechanical properties of dental resin-composites. Dent Mater 2012;28:1292–300.
[36] Lai H, Lin X, Zhang Y, Gong Q, Tong Z. Effect of different endodontic access preparations on the biomechanical behavior of lithium disilicate and resin nanoceramic onlay restorations: An in vitro and 3D finite element analysis study. J Prosthet Dent 2022.
[37] Aparna J, Maiti S, Jessy P. Polyether ether ketone - As an alternative biomaterial for Metal Richmond crown-3-dimensional finite element analysis. J Conserv Dent 2021;24:553–7.
[38] Sinha N, Thompson GA, Drago C, An H. Shear bond strength characteristics on surface treatment modalities of CAD-CAM resin polymers. J Prosthodont 2023.
[39] Papathanasiou I, Kamposiora P, Dimitriadis K, Papavasiliou G, Zinelis S. In vitro evaluation of CAD/CAM composite materials. J Dent 2023;136:104623.
[40] Jeong H-Y, Lee H-H, Choi Y-S. Mechanical properties of hybrid computer-aided design/computer-aided manufacturing (CAD/CAM) materials after aging treatments. Ceram Int 2018;44:19217–26.
[41] Heintze SD, Monreal D, Reinhardt M, Eser A, Peschke A, Reinshagen J, et al. Fatigue resistance of all-ceramic fixed partial dentures - Fatigue tests and finite element analysis. Dent Mater 2018;34:494–507.
[42] Ausiello P, Ciaramella S, Di Rienzo A, Lanzotti A, Ventre M, Watts DC. Adhesive class I restorations in sound molar teeth incorporating combined resin-composite and glass ionomer materials: CAD-FE modeling and analysis. Dent Mater 2019;35:1514–22.
[43] Askerbeyli Örs S, Serper A. Influence of nickel-titanium rotary systems with varying tapers on the biomechanical behaviour of maxillary first premolars under occlusal forces: a finite element analysis study. Int Endod J 2018;51:529–40.
[44] Cağlar A, Aydin C, Ozen J, Yilmaz C, Korkmaz T. Effects of mesiodistal inclination of implants on stress distribution in implant-supported fixed prostheses. Int J Oral Maxillofac Implants 2006;21:36–44.
[45] Yamanel K, Çağlar A, Gülşahi K, Özden UA. Effects of different ceramic and composite materials on stress distribution in inlay and onlay cavities: 3-D finite element analysis. Dent Mater J 2009;28:661–70.
[46] Tatarciuc M, Maftei GA, Vitalariu A, Luchian I, Martu I, Diaconu-Popa D. Inlay-retained dental bridges—a finite element analysis. Appl Sci 2021;11:3770.
[47] Tribst JPM, Dal Piva AMO, de Melo RM, Borges ALS, Bottino MA, Özcan M. Short communication: Influence of restorative material and cement on the stress distribution of posterior resin-bonded fixed dental prostheses: 3D finite element analysis. J Mech Behav Biomed Mater 2019;96:279–84.
[48] Kuijs R, van Dalen A, Roeters J, Wismeijer D. The resin-bonded fixed partial denture as the first treatment consideration to replace a missing tooth. Int J Prosthodont 2016;29:337–9.
[49] Alraheam IA, Ngoc CN, Wiesen CA, Donovan TE. Five-year success rate of resin-bonded fixed partial dentures: a systematic review. J Esthet Restor Dent 2019;31:40–50.
[50] Tortopidis D, Lyons MF, Baxendale RH, Gilmour WH. The variability of bite force measurement between sessions, in different positions within the dental arch. J Oral Rehabil 1998;25:681–6.
[51] Bakke M, Michler L, Möller E. Occlusal control of mandibular elevator muscles. Scand J Dent Res 1992;100:284–91.
[52] Dal Piva AM de O, Tribst JPM, Borges ALS, Souza RO de Bottino A e. CAD-FEA modeling and analysis of different full crown monolithic restorations. Dent Mater 2018;34:1342–50.
[53] Najeeb S, Zafar MS, Khurshid Z, Siddiqui F. Applications of polyetheretherketone (PEEK) in oral implantology and prosthodontics. J Prosthodont Res 2016;60:12–9.
[54] Subaşı MG, Çakmak G, Sert M, Yilmaz B. Effect of multiple firings on surface roughness and flexural strength of CAD-CAM ceramics. J Prosthet Dent 2022;128:216.e1–8.
[55] Elraggal A, Afifi R, Abdelraheem I. Effect of erosive media on microhardness and fracture toughness of CAD-CAM dental materials. BMC Oral Health 2022;22:191.
[56] Li W, Swain MV, Li Q, Ironside J, Steven GP. Fibre reinforced composite dental bridge. Part I: Experimental investigation. Biomaterials 2004;25:4987–93.
[57] Kermanshah H, Geramy A, Ebrahimi SF, Bitaraf T. IPS-empress II inlay-retained fixed partial denture reinforced with zirconia bar: three-dimensional finite element and in-vitro studies. Acta Odontol Scand 2012;70:569–76.
[58] Mainjot A. Recent advances in composite CAD/CAM blocks. Int J Esthet Dent 2016;11:275–80.
[59] Leung BTW, Tsoi JKH, Matinlinna JP, Pow EHN. Comparison of mechanical properties of three machinable ceramics with an experimental fluorophlogopite glass ceramic. J Prosthet Dent 2015;114:440–6.
[60] Mesquita RV, Axmann D, Geis-Gerstorfer J. Dynamic visco-elastic properties of dental composite resins. Dent Mater 2006;22:258–67.
[61] El-Damanhoury HM, Haj-Ali RN, Platt JA. Fracture resistance and microleakage of endocrowns utilizing three CAD-CAM blocks. Oper Dent 2015;40:201–10.
[62] Dejak B, Mlotkowski A. Three-dimensional finite element analysis of strength and adhesion of composite resin versus ceramic inlays in molars. J Prosthet Dent 2008;99:131–40.
[63] Rathmann F, Bömicke W, Rammelsberg P, Ohlmann B. Veneered zirconia inlay-retained fixed dental prostheses: 10-Year results from a prospective clinical study. J Dent 2017;64:68–72.